Environmental Pollution 206 (2015) 390–399

Contents lists available at ScienceDirect

Environmental Pollution

journal homepage: www.elsevier.com/locate/envpol

Modelling of oil spills in confined maritime basins: The case for early response in the Eastern Mediterranean Sea

Tiago M. Alves [a, *], Eleni Kokinou [b], George Zodiatis [c], Robin Lardner [c], Costas Panagiotakis [d], Hari Radhakrishnan [c]

[a] 3D Seismic Lab, School of Earth and Ocean Sciences, Cardiff University, Main Building-Park Place, Cardiff CF10 3AT, United Kingdom
[b] Department of Environmental and Natural Resources Engineering, Technological Educational Institute Crete, 3 Romanou Str. Chalepa, Chania, Crete GR 73133, Greece
[c] Oceanography Centre, University of Cyprus, P.O. Box 20537, 1678 Nicosia, Cyprus
[d] Department of Business Administration, Technological Educational Institute Crete, Agios Nikolaos, Greece

ARTICLE INFO

Article history:
Received 1 June 2015
Received in revised form
23 July 2015
Accepted 25 July 2015
Available online xxx

Keywords:
Eastern Mediterranean
Oil spill simulations
Oceanography
Bathymetry
Chemical dispersants

ABSTRACT

Oil spill models are combined with bathymetric, meteorological, oceanographic, and geomorphological data to model a series of oil spill accidents in the Eastern Mediterranean Sea. A total of 104 oil spill simulations, computed for 11 different locations in the Levantine Basin, show that oil slicks will reach the coast of Cyprus in four (4) to seven (7) days in summer conditions. Oil slick trajectories are controlled by prevailing winds and current eddies. Based on these results, we support the use of chemical dispersants in the very few hours after large accidental oil spills. As a corollary, we show shoreline susceptibility to vary depending on: a) differences in coastline morphology and exposure to wave action, b) the existence of uplifted wave-cut platforms, coastal lagoons and pools, and c) the presence of tourist and protected environmental areas. Mitigation work should take into account the relatively high susceptibility of parts of the Eastern Mediterranean.

1. Introduction

Oil spills in remote offshore regions are of difficult management due to their relative distance to the shore, where civil protection teams and clean-up equipment are located. In addition, a strong influence of seasonal oceanographic and weather conditions is usually recorded offshore (Doerffer, 1992; Anderson and LaBelle, 2000; Burgherr, 2007). Key examples of this influence have been witnessed during the M/V Exxon Valdez (1989) and M/V Prestige (2002) accidents. Both accidents recorded the scattering and beaching of oil by strong currents and winds through a vast area (Petterson et al., 2003; González et al., 2006). Recent data on the Gulf of Mexico, Baltic and West Mediterranean Seas confirmed the crucial effect variable weather and oceanographic conditions have on oil slick movement and biodegradation (e.g., Cucco et al., 2012; Soomere et al., 2014; Prince, 2015).

Important re-circulation and scattering of oil by natural processes occurred during the Deepwater Horizon spill of 2010 (Atlas and Hazen, 2011; Thibodeaux et al., 2011). During its mitigation, real-time modelling of chemically dispersed oil under variable weather and oceanic conditions was paramount to the monitoring of ensuing environmental impact(s). For instance, the anionic surfactant DOSS (dioctyl sodium sulfosuccinate) included in chemical dispersants was found to be sequestered in deepwater hydrocarbon plumes at 1000–1200 m water depth. DOSS recorded a conservative transport and dilution (<1 ppm of oil) at depth, but persisted up to 300 km from the Deepwater Horizon platform some 64 days after dispersant applications ceased into the flow of oil near the seafloor (Kujawinski et al., 2011). Importantly, DOSS was selectively associated with the oil and gas phases in the deepwater plume, but recorded negligible (or slow) rates of biodegradation in the affected waters. DOSS concentrations and dispersant-to-oil ratios were lower than those tested in published toxicology data, but hint at significant movement of other hydrocarbon solvents in the water column after major oil spills (Kujawinski et al., 2011).

In the Baltic and Western Mediterranean Seas, statistical analyses of oil spill trajectories allowed the identification of areas

* Corresponding author.
E-mail addresses: alvest@cardiff.ac.uk (T.M. Alves), ekokinou@chania.teicrete.gr (E. Kokinou), gzodiac@ucy.ac.cy (G. Zodiatis), cpanag@staff.teicrete.gr (C. Panagiotakis).

http://dx.doi.org/10.1016/j.envpol.2015.07.042

where the impact of spilt oil is more significant (Chrastansky and Calles, 2009; Soomere et al., 2010; Lu et al., 2012; Olita et al., 2012; Soomere et al., 2014). These same statistical analyses confirmed the unpredictability of oil spill movement in extreme weather conditions, and the sensitivity of deterministic circulation models to small variations in the initial and forcing conditions (Griffa et al., 2004; Ciappa and Costabile, 2014). The understanding of small variations in circulation models was recognised by the latter authors as being paramount in the management of civil protection teams, often with limited resources and equipment, during the mitigation of large oil spill accidents.

As with the Gulf of Mexico, Baltic and Western Mediterranean regions, the variable weather conditions known to the Eastern Mediterranean Sea make the real-time prediction of oil spill movement crucial to prevent and mitigate major pollution events. Comprising one of the busiest shipping corridors in the world (REMPEC, 2002), weather and sea current patterns in the Eastern Mediterranean can vary significantly from summer to winter, and during storms, at times hindering mitigation procedures from civil protection authorities (POEM Group, 1992; Pinardi et al., 2006; Zodiatis et al., 2005, 2010; 2013; Menna et al., 2012). Challenging weather conditions can also be recorded during summer, as shown recently in the Ammochostos Bay. The northern part of Ammochostos Bay in Cyprus experienced a spill of 100 tonnes of heavy oil with 26° API, on 15 July 2013, during the upload of crude oil from a tanker in strong breeze (Beaufort 6) conditions (https://weatherspark.com/history/32006/2013/Larnaca-Cyprus). Large oil spills in challenging weather conditions were also recorded offshore Greece in the Bay of Pylos (1980), in Lefkandi and Kythira (2000) and in smaller, but rather common, accidents in the Aegean Sea (Giziakis et al., 2013). The largest platform accident in the Eastern Mediterranean was the 2004 Adriatic IV jack-up rig explosion, in which no oil spill ensued (Vinnem, 2014). In contrast, the bombing of the Jiyeh power station in Lebanon in 2006 resulted in the release of 15,000–20,000 tonnes of oil (Coppini et al., 2011). In the Eastern Mediterranean region, the importance of oil spills is enhanced when considering acute pollution events such as the Lebanon 2006 oil spill, or potential collision accidents in what is a major route for oil and gas tankers from the Middle East to Europe and North America (UNEP/MAP, 2012).

This paper presents the results of 104 new oil spill simulations, bathymetric analyses and shoreline susceptibility maps for the region spanning the Mediterranean coasts of Cyprus, Egypt, Israel, Lebanon, Syria and Turkey (Fig. 1a). The aim is to understand oil spill movement and scattering in offshore regions where exploration drilling has been equated, or has occurred in the past, so that the best practices are suggested to civil protection authorities in the Eastern Mediterranean (and other confined seas) to control, and clean, remote oil spills, either maritime or platform related. In summary, this work addresses the following questions:

a) How quickly spilt oil will reach the Eastern Mediterranean shores under known oceanographic and meteorological conditions?
b) In what direction(s) spilt oil will be dispersed before reaching the shore, and for how long it will remain at sea?
c) In light of the new model results what will be the best mitigation techniques to prevent large quantities of oil reaching the Eastern Mediterranean shores?

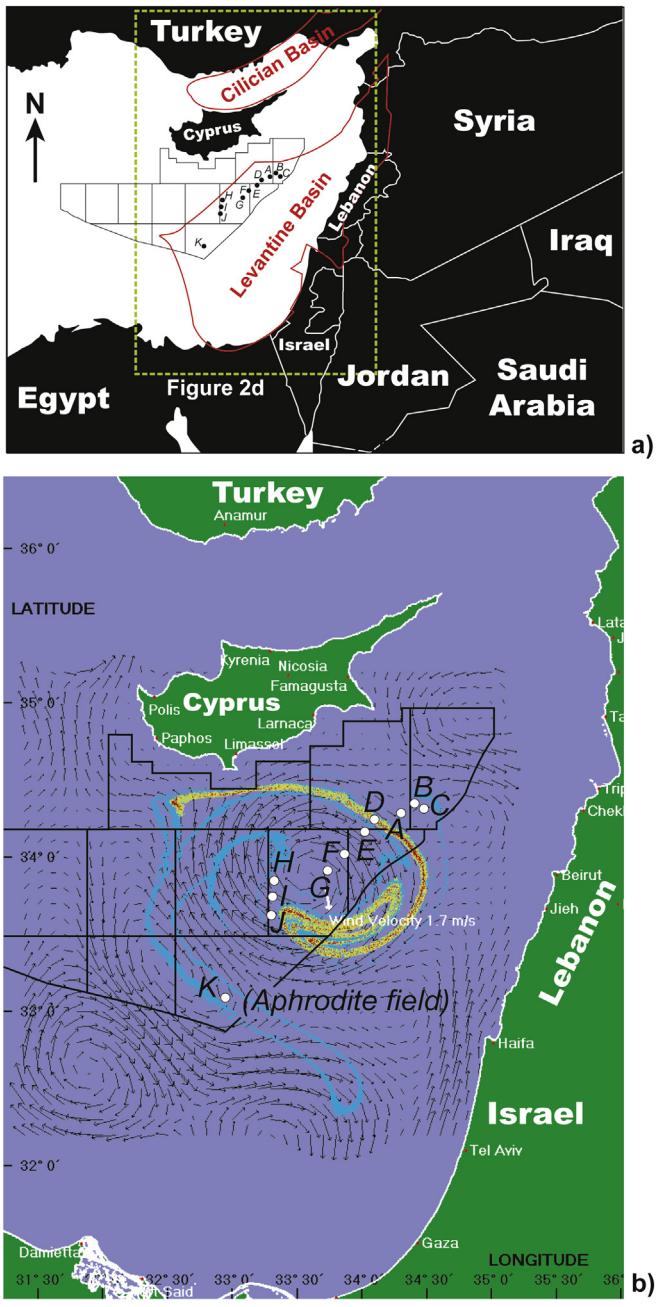

Figure 1

Fig. 1. (a) Location map showing the study area relative to the Cilician and Levantine Basins, Eastern Mediterranean Sea. The area analysed in this work is highlighted by the green box. The geometric areas south of the island of Cyprus highlight current hydrocarbon exploration blocks south of Cyprus. Locations A to K are also shown in the figure. (b) MEDSLIK model of slick diffusion under late spring conditions (01 June 2013 to 30 June 2013) for an oil spill accident originated at the Aphrodite field. The model considered a release of Belayim oil (API 23.5°) for 50 days, at a rate of 8000 m^3/day. Average wind velocities of 1.7 m/s blow in a northerly direction during the accident. The model shows that surface currents will cause widespread scattering of the oil slick by current eddies. Locations A to K, as well as hydrocarbon exploration blocks south of Cyprus, are highlighted in the figure. (For interpretation of the references to colour in this figure legend, the reader is referred to the web version of this article.)

2. Datasets and methods

The data in this paper were analysed using the methodology in Lardner and Zodiatis (1998), which was updated to accommodate the processing of bathymetry data for the Eastern Mediterranean Sea (see Section 3). Physical parameters, such as wind direction, ocean circulation and wave direction were taken into account in the models compiled, as illustrated in Supplementary Fig. 1. In summary:

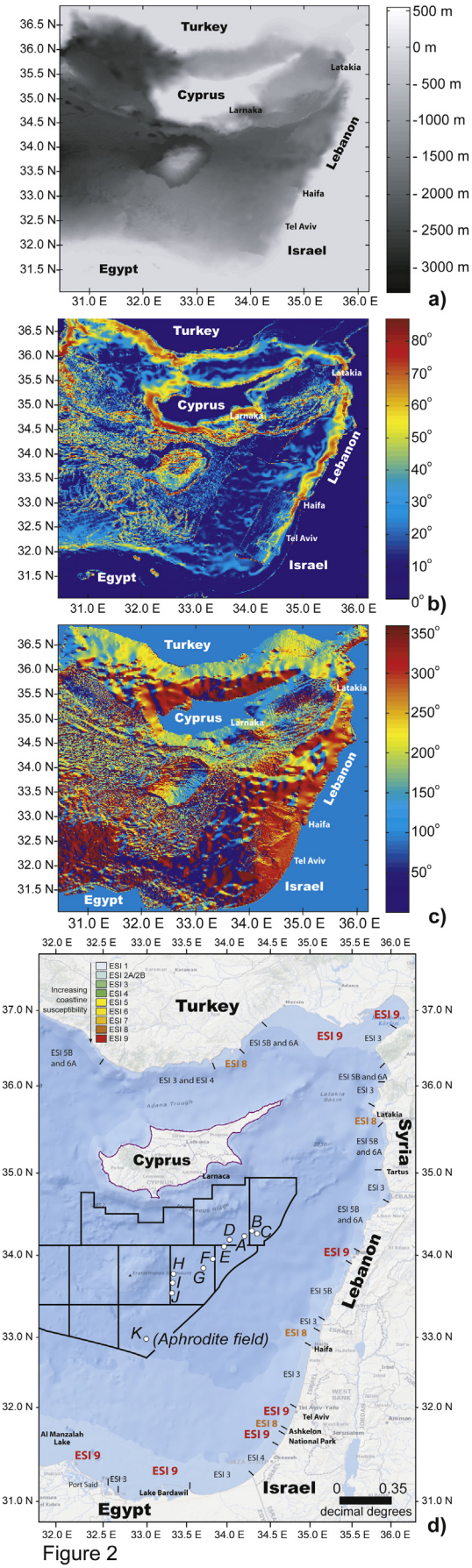

Figure 2

1) Bathymetry, geomorphology, meteorological and oceanographic conditions were considered in a first stage as the main factors controlling the movement of oil slicks in the Eastern Mediterranean Sea. Sea-bottom morphology in the study area is complex, and has a close influence on ocean circulation (Fig. 2a and b). For this reason we considered appropriate to analyse bathymetric data using modern Linear Pattern Detection techniques (e.g. Panagiotakis and Kokinou, 2015).
2) Oil movement was simulated in a second stage using Mediterranean Oil Spill and Floating Objects Prediction (MEDSLIK) models (Lardner and Zodiatis, 1998; Lardner et al., 2006; Zodiatis et al., 2012). The models were compiled using high temporal and spatial resolution data for wind, wave, sea surface temperature and 3D sea current conditions provided by the Cyprus Coastal Ocean Forecasting and Observing System (CYCOFOS) for the period January 2010 to January 2013. Also estimated by the oil spill models were the percentage volumes of oil evaporated, dispersed and trapped in Eastern Mediterranean shores.

2.1. Step 1 – integration of bathymetric, geomorphological and geological data

For the purposes of this work, the coastline morphology was determined from the ArcGIS 10 online database, whereas local morphological data were derived from Google Maps®. The primary aim was to check the effect of seabed morphology on ocean circulation and, especially, the presence of strong gyres in the study area. Also important was to access the impact of oil spills on sea-bottom features, urban areas with important infrastructures, and tourism sites and coastal regions showing high susceptibility to oil pollution due to their morphology and presence of environmentally protected areas (Natura 2000 sites, http://cdr.eionet.europa.eu/gr/eu/n2000/envujeg6w).

Land and sea elevation data for the wide area of Cyprus come from the ArcGIS 10 online database. Bathymetric data from the European Marine Observation and Data Network (EMODNET) concerning the Levantine Basin (Berthou et al., 2008) were also used (Fig. 2a). Data resolution approaches a grid size of ¼ by ¼ arc minutes i.e., 0.4 by 0.4 km at 31°N. The World Geodetic System 84 (WGS84) was the chosen geodetic system for the bathymetric data, and other geographically referenced information. This latter information included bathymetry layers with the average, minimum, maximum, standard deviation and smooth water depths in metres to latitude (LAT).

Bathymetric data were processed in MATLAB by applying a new algorithm for the automatic enhancement and identification of linear patterns that relate to important geomorphological features (Panagiotakis and Kokinou, 2015) (Fig. 2a and b). According to this method, the slope and aspect images are computed together with their derivatives. A rotation and scale-invariant filter and pixel-labelling methods are then applied to enhance the detection of geomorphological features.

Fig. 2. (a) Bathymetric data from the Eastern Mediterranean as compiled from EMODNET data. (b) Slope map of the Eastern Mediterranean as compiled from EMODNET bathymetric data. (c) Aspect map computed from EMODNET bathymetric data following the methodology described in this paper. (d) Shoreline susceptibility map showing in red the regions of higher susceptibility in the Eastern Mediterranean. The map was compiled using open-file geological maps and shoreline morphological analyses based on Google Earth®. Main cities and modelled oil spill Locations A to K are highlighted on the map. See Table 1 and Adler and Inbar (2007) for a detailed description of types ESI 1 to ESI 9 in terms of shoreline susceptibility. Locations A to K and current hydrocarbon exploration blocks from offshore Cyprus are shown in the figure. (For interpretation of the references to colour in this figure legend, the reader is referred to the web version of this article.)

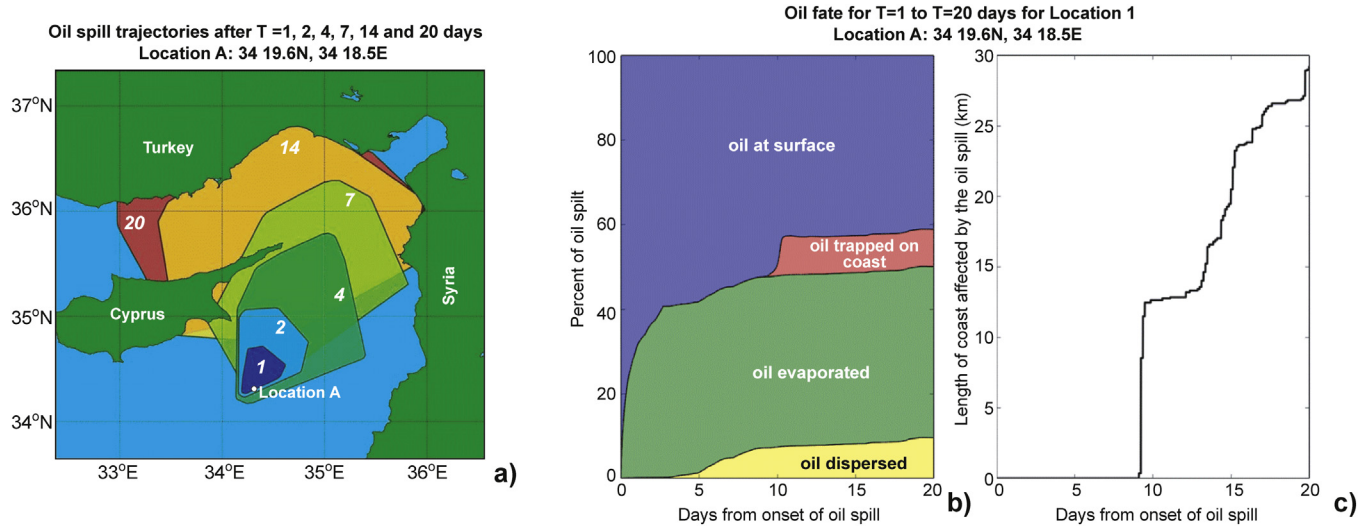

Fig. 3. (a) Superimposed oil spill trajectory model for T = 1, 2, 4, 7, 14 and 20 days, as computed on MEDSLIK for summer conditions. Numbers within the coloured areas indicate days after the oil spill accident in Location A. (b) Graph showing the percentages of oil evaporated, dispersed, trapped on coast, free on coast, and at the sea surface for the oil spill in Location A considered in the MEDSLIK model. (c) Length of the coastline affected by the spill for the same oil spill for the time-period considered in the model (T = 20 days).

2.2. Step 2 – MEDSLIK oil spill predictions

Three-dimensional data for sea currents and sea-surface temperatures from CYCOFOS were used in the MEDSLIK oil spill predictive models. The CYCOFOS includes data within a 1-km grid, covering the NE part of the Levantine Basin and the Exclusive Economic Zone (EEZ) of Cyprus. High frequency, hourly wind data were obtained from the SKIRON regional weather forecasting model for the Mediterranean Sea run at the University of Athens with a 5 by 5-km horizontal resolution (http://forecast.uoa.gr/forecastnewinfo.php). In parallel, this work used 3-hourly wave data, obtained from CYCOFOS, with a 5 by 5-km horizontal resolution (Lardner, 2013). MEDSLIK was used in its latest operational version 5.4.0 (Lardner and Zodiatis, 1998; Lardner et al., 2006; Zodiatis et al., 2012; Lardner, 2013). MEDSLIK is a 3D oil-spill model that is able to predict the transport, fate and weathering of oil slicks at any given offshore location and depth from the source of oil pollution – upon the availability of oceanographic and weather data.

In this paper, MEDSLIK simulations were compiled for the four seasons in each year, from January 2010 to January 2013. Volumes of oil dispersed, evaporated, at the coast and at the surface were modelled for the 11 locations A to K shown in Fig. 1a and b. The total volume of oil released on the sea surface was 55,800 barrels (bbls) of medium grade oil for all scenarios, which were re-initiated every 15 days. We chose medium grade oil based on the type found in the Suez region and Northern Egypt e.g., Ashrafi Field with API values between 35 and 38° (Metwalli et al., 2012). The MEDSLIK models computed oil spill simulations for periods of 20 days. A total of 104 oil spill simulations were performed for each of the 11 locations (see Fig. 1). Emulsification was simulated and viscosity changes in the spilt oil were computed according to the amounts of emulsification and evaporation.

For all 104 simulations were derived average concentrations of oil. Also calculated were the minimum time for the oil spill to reach the shoreline, and the average amount of oil expected on the shoreline. Based on the above data, we selected in this paper the scenarios with the maximum amount of oil on the shoreline, and calculated the length of the coast affected by oil. Thus, we analyse in this paper the worst-case scenarios for each oil spill location.

In a final step, we compiled superposition maps for the worst-case scenarios considered, for 1–2–4–7–14–20 days (Fig. 3a and Supplementary Fig. 2). The superposition maps show the maximum distance travelled by the oil spill under known weather conditions. MEDSLIK also computed plots of Oil Fate Parameters, i.e. the volume percentages of oil afloat, evaporated, trapped on the coast, dispersed and emulsified (Fig. 3b and c). In this paper, we compare and contrast data for winter and summer conditions, in weeks 0–10 and 26 to 36 of each calendar year.

2.3. Step 3 – compilation of shoreline susceptibility maps and cross-correlation with oil spill models

A new shoreline susceptibility map was compiled for the Eastern Mediterranean using the Environmental Susceptibility Index (ESI) proposed by Adler and Inbar, 2007 (Fig. 2d). The ESI classification considers a range of values between 1 and 9, with level 1 (ESI 1) representing areas of low susceptibility, impermeable to oil spilt during accidents, such as linear shorelines with rocky cliffs. In contrast, ESI 9 shores are highly vulnerable, and often coincide with natural reserves and special protected areas (Lardner and Zodiatis, 1998). We used GoogleMaps® and geological maps to highlight the key coastal regions to protect in case of offshore oil spill accidents. Details of the ESI classification (Adler and Inbar, 2007) are given in Table 1.

3. Results

3.1. Offshore bathymetry

Bathymetric features are able to alter ocean circulation and oil spill trajectories in offshore oil spills (Marshall, 1995; Whitehead, 1998; Gille et al., 2004). The Eastern Mediterranean Sea presents a complex bathymetry, which is shown in Fig. 2a. Water depth north of the Cyprus Arc reaches 1500 m, whereas south of the same arc water depths reach up to 3500 m (Fig. 2a).

Submarine geomorphological features were highlighted in our analyses by compiling slope and aspect maps from bathymetric data (Fig. 2b). Slopes to the south of the Cyprus Arc are generally steep and exceed 40° at places (Fig. 2b). The coastal part of Cyprus presents a smoother relief, with slopes ranging between 0°-30°. South of the Cyprus Arc, and especially in the area of the Eratosthenes Seamount, slopes present the whole range of dips (Fig. 2b).

Table 1
Shoreline Environmental Susceptibility Index (ESI) as defined in Adler and Inbar (2007), representing the susceptibility of particular types of coasts to offshore oil spills.

Environmental sensitivity Index (ESI)	Shoreline type	Main features and characteristics
ESI 1	Natural, vertical exposed rocky cliffs or headlands; or vertical manmade sea-walls or structures exposed to the open sea	Exposed to the open sea; impermeable to oil; high natural cleanup ability
ESI 2A	Flat abrasion wave cut platforms	Exposed to high wave energy; impermeable to oil (except for very calm and low tide conditions); high natural cleanup ability
ESI 2B	Flat, coarser or slightly sloping exposed platforms created by waves; or low, exposed rocky beaches with larger rocky boulders or structures	Mildly sloping platforms, mostly impermeable to oil; quite high natural cleanup ability
ESI 3	Fine to medium grained sandy beaches, mostly moderately sloping	Low to medium penetration of oil (especially in warm weather); exposed beaches; medium to high natural cleanup ability
ESI 4A	Coarse grained sandy beaches, mostly with a steeper slope	Medium penetration and burial of oil; medium natural cleanup ability
ESI 4B	Artificial building material dump and/or mixed gravel and small boulders	Low 'environmental value' (dump sites of building material); high penetration and burial by oil. Often, oil traps
ESI 5A	Beaches with mixtures of coarse sand, gravel, pebbles and/or shells	Medium to high penetration and burial of oil
ESI 5B	Irregular protrusions of rocks through sand, shells or gravel; or any other irregular, coarse mixture of rocks and unconsolidated sediments	Oil traps in irregular features; medium to high penetration of oil. Limited natural cleanup ability
ESI 6A	Gravel and pebble beaches	Deep penetration and burial of oil (especially in warm weather); exposed to the open sea and high wave energy; limited natural cleanup ability
ESI 6B	Man-made, exposed breakwaters extended to the open sea, built of large rocks, rip-rap, or concrete 'tetrapodes' or man-made rip rap structures on the beach for coastal protection	High penetration of oil in cracks between boulders, often a trap for large quantities of oil. The side facing the open sea has a high natural cleanup ability. If oil penetrates to sheltered areas of the harbour - low natural cleanup ability
ESI 7	Small rivers outlets and 'wet' sandy beaches by high ground water	Low penetration of oil; high biological productivity; mostly exposed to the open sea; possible entrance of oil into the rivers
ESI 8	Ports and marinas protected by breakwaters or rocky beaches which are protected, or unexposed to the open sea	Areas sheltered from the open sea; Irregular surfaces and morphologies. Often traps for large quantities of oil
ESI 9	Beaches with high environmental or biological importance or beaches with other high sensitivity or importance	Nature reserves, especially protected areas, intakes of cooling water for power stations, etc.

The eastern part of the Levantine Basin shows a different morphology, comprising a generally flat region with slopes between 0° and 20°. This morphology changes towards the continental slopes of Israel and Lebanon where a steep continental slope is observed (Fig. 2b).

Prevailing aspects north of the Cyprus Arc are in the range of 157°–202° (south) to 112°–157° (southeast) (Fig. 2c). The areas corresponding to the Larnaca-Latakia and Hecateous ridges differ from the previous pattern, showing aspects mostly oriented north (0°–22°) and northeast (22°–67°). In the area between the Cyprus Arc and the Eratosthenes Seamount, south (157°–202°) aspects generally prevail. A completely different distribution of aspects dominates south of the Eratosthenes Seamount. The prevailing aspect orientation is north (0°–22°) and northwest (292°–337°) to northeast (22°–67°).

Predominant currents, gyres and eddies are strongly controlled by the general thermohaline pattern of the Eastern Mediterranean (POEM Group, 1992; Pinardi et al., 2006; Zodiatis et al., 2005, 2010; 2013), while the upper surface layer of the circulation is affected by the strong wind fields, particularly northwesterly and southwesterly winds (Menna et al., 2012). Fig. 1b shows the oil slick trajectory under late spring conditions for an accident originated at the Aphrodite field, and sea surface currents recorded in this area during the time period considered in the model. Fig. 2a–c correspond to the bathymetry analyses undertaken in this paper. In particular, oil spill trajectories off the southern coast of Cyprus are related to the presence of the Eratosthenes Seamount, where large variations in bathymetric parameters are observed.

3.2. Coastal geomorphology

The Eastern Mediterranean is dominated by a straight, low-lying shoreline in its southern and southeastern parts and by a complex morphology to the north and northeast (Figs. 2a and 3). This complex morphology relates to Late Cenozoic tectonics, which uplifted some stretches of the coastline while causing subsidence in others (Fingas, 2011). Significant changes in the nature of shoreline sediments, and underlying geological units, are also reflected in changes in shoreline morphology, namely in the formation of coastal spits and bays in the northeastern part of the study area.

A relatively straight coastline is observed in the region spanning the Al-Manzalah Lake (Egypt) to central Israel (Fig. 3). However, coastal lagoons and natural reserves make this stretch of coastline susceptible to trapping oil. The largest coastal lake in the region is located east of the Nile Delta in the hypersaline Lake Bardawil (El-Bana et al., 2002) (Fig. 2c). A simple linear coastline is observed from Lake Bardawil to Haifa, in northern Israel (Fig. 2d), where most of this coastline is exposed to wave action (Zodiatis et al., 2012).

Spits and bays are common from Haifa to the north, where rocky shorelines are also common, This morphology is maintained in Syria and Turkey, although interrupted by linear stretches of low-lying beaches south of Tartus (Syria), Latakia (Syria) and on linear shores in southern Turkey (Fig. 2c and d).

3.3. Coastline susceptibility mapping

Field data from Cyprus show higher susceptibility values (ESI 9 and ESI 8) in regions where demographic pressure is higher, or where natural pools and artificial barriers favour the trapping of oil near the coast (e.g. Alves et al., 2016). This same trend is observed in the entire Eastern Mediterranean region, with a clear divide occurring at the latitude of Haifa (Fig. 2d). To the south of Haifa susceptibility values are limited to ESI 3 to ESI 4 through most part of the coast, the exceptions being the Ashkelon National Park in Israel and costal lagoons in Egypt in which ESI values are high (Fig. 2d). To the North of Haifa there is a marked variability in ESI

values, but with significant areas of the shoreline reaching values of ESI 8 and ESI 9 (Fig. 2d).

An important factor controlling shoreline susceptibility is the presence of natural oil traps in the form of (protected) coastal lagoons and uplifted beaches with natural pools and spits. In particular, salt marshes and coastal lakes can draw water from foreshore areas polluted with oil, contaminating sub-surface aquifers and soil for a long time after an oil spill. Protected sandy shorelines, with fine sands and muds deposited over older friable sediment of high porosity and sheltered from wave action, are also sites of enhanced susceptibility, particularly when close to large cities, tourist resorts or natural reserves (Fig. 2c).

4. Modelled scenarios for distal offshore spills

Fig. 3a–c shows oil fate scenarios for oil spilt from Location A for summer conditions (weeks 26–36), together with graphs showing percentage volumes of dispersed, evaporated, trapped and surface oil, one (1) to twenty (20) days after the onset of the oil spill. As shown in Fig. 3a, the most vulnerable areas in the event of a 55,800 bbls medium-grade oil spill are the Syrian, Turkey and east Cyprus coastlines, which will be affected four (4) to fourteen (14) days after the onset of the oil spill if no clean-up and mitigation procedures are implemented. In particular, the eastern shore of Cyprus will be affected some four (4) to seven (7) days after the oil spill accident in Location A, polluting a stretch of coast >30 km by day 20 (Fig. 3a–c).

A complete series of oil movement maps were compiled for accidents in Locations A to J, as shown in Figs. 4 and 5. Oil movement maps were compiled on MEDSLIK for winter (weeks 0–10) and summer (weeks 26–36) conditions. In eight of the ten oil spill locations examined for winter conditions, the first impact on the coast will be recorded on the east coast of Cyprus eight (8) to fourteen (14) days after the onset of the spill accident (Fig. 4). Oil spills in Locations I and J record the first impacts on the shoreline of Lebanon, ~14 days after the oil spill started.

A distinct setting is recorded for summer conditions (weeks 26–36), under which oil will preferentially drift northwards under prevailing southwesterly and southerly winds (Paschardes and Christofides, 1995). The MEDSLIK models show oil slicks arriving in SE and E Cyprus in days 4–7 when sourced from Locations A to F (Fig. 5a–f). In contrast, MEDSLIK models suggest an early eastward to northeastward drift of oil slicks sourced from Locations G to J. Only after day 4 is recorded a marked northward drift in the slicks, with adjacent coastlines being polluted between days 7 and 14, or even after day 14 in the case of Location J (Fig. 5).

An important observation from the spill superposition maps is the quick drift of oil after day 2 in all modelled cases (Figs. 4 and 5). The drifting of oil also occurs in distinct directions. Winter conditions denote a predominant north to northeast drift of oil, but local winds and currents can transport oil slicks to the southwest in Locations A to D, thus retarding the arrival of oil to the shore (Fig. 4). Differences between summer and winter conditions are markedly felt in terms of the speed in which the slicks drift (Figs. 4 and 5).

In the case of Locations A to E, oil slicks will potentially reach the coast of Southern Cyprus four (4) days after an oil spill accident in summer conditions (Fig. 5). This shows a much reduced time period for civil protection authorities to initiate their cleaning operation in the summer, when compared with winter conditions (Figs. 4 and 5). The exception to this rule are oil spills in Locations G to J, in summer conditions, which present an early drift towards the east and northeast, leading to a later arrival of oil slicks to the Cyprus, Lebanon, Syria and Israel coasts.

5. Discussion

5.1. Oil scattering patterns in the Eastern Mediterranean Sea

The data presented in this paper provide evidence of the scale and distribution of oil slicks subject to distinct weather conditions. There are, however, common results from the 104 oil spills simulations:

a) Under typical summer conditions, Eastern Mediterranean shores record the arrival of oil four (4) to seven (7) days after the onset of the oil spill accident.
b) Meteorological and oceanographic conditions will be important at first, but the general result of the models is the progressive movement of oil towards the north and northeast in both summer and winter conditions.
c) Oil slicks will be influenced by wind conditions in the first two (2) days after the spill, but will invariable affect the Cilician and northern Levantine basins by day 14.

The accurate knowledge of the potential extreme wind speed and wave height values over an area of interest is of critical importance for oil spill monitoring. In the presence of elevated wind speeds, wind conditions dominate over all the other components that affect the oil spill evolution, determining the movement of the slick. In detail, winds of 2–7 m/s impact heavily close to the spill source, and quick oil spill scattering is expected with strong winds and swells (Coppini et al., 2011). Furthermore, the effectiveness of applying dispersant to oil spills is influenced by wind as the amount of dispersant that contacts the target is highly dependent on local wind- and sea turbulence conditions (Nissen et al., 2010).

The Levantine Basin and, in particular, the area south of Cyprus have been identified as regions where extreme winds can be frequently recorded (Galanis et al., 2012). Confirming and further specifying this fact, Zodiatis et al. (2014) developed a 10-year very-high resolution hindcast analysis, which showed the area south of Cyprus to be characterised by westerly winds and waves, and exposed to swell waves of relatively low heights. Possible extreme values have been estimated to approximately 10 m/sec for wind speed and to 2 m for significant wave height based on their probability distributions. It is worth noticing that the general distribution of wind and wave values in the Levantine Basin is strongly influenced by extreme events. Previous 50-year wind data analyses over the area of Cyprus (Pashardes and Christofides, 1995) concluded that high values of wind speed are common during winter, with prevailing directions varying from south to southwest during daytime and from northwest to northeast during the night. In particular, wind at coastal locations can achieve speeds of over 15 m/s with the hourly mean values up to 20 m/s. The variations in wind velocity can be as much as 10 m/s between mean values recorded every hour.

5.2. Advantages and disadvantages of chemical vs. mechanical removal

When selecting the most effective mitigation techniques for oil spilt in the Levantine Basin, one key issue under consideration by civil protection authorities relates to the velocity in which the slick is expected to scatter and move. Most of the MEDLIK models for Locations A to J show a period of four (4) to seven (7) days in summer conditions, and eight (8) to fourteen (14) days under typical winter conditions, to mitigate the oil slicks before they reach the shore. Importantly, the scattering of individual slicks through the Levantine Basin can challenge the best mitigation

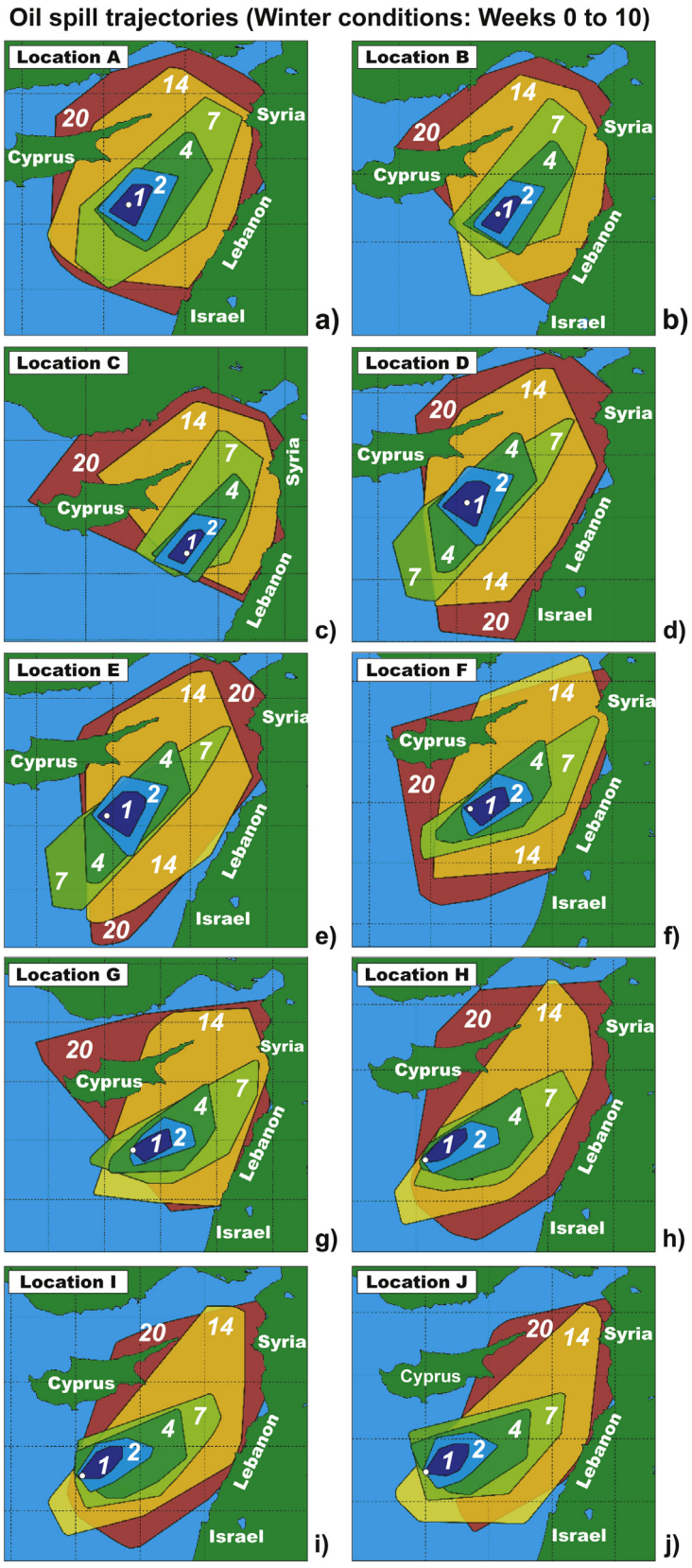

Fig. 4. Superimposed oil spill trajectory maps for T = 1, 2, 4, 7, 14 and 20 days, as computed on MEDSLIK. The figure corresponds to winter conditions (weeks 0–10).

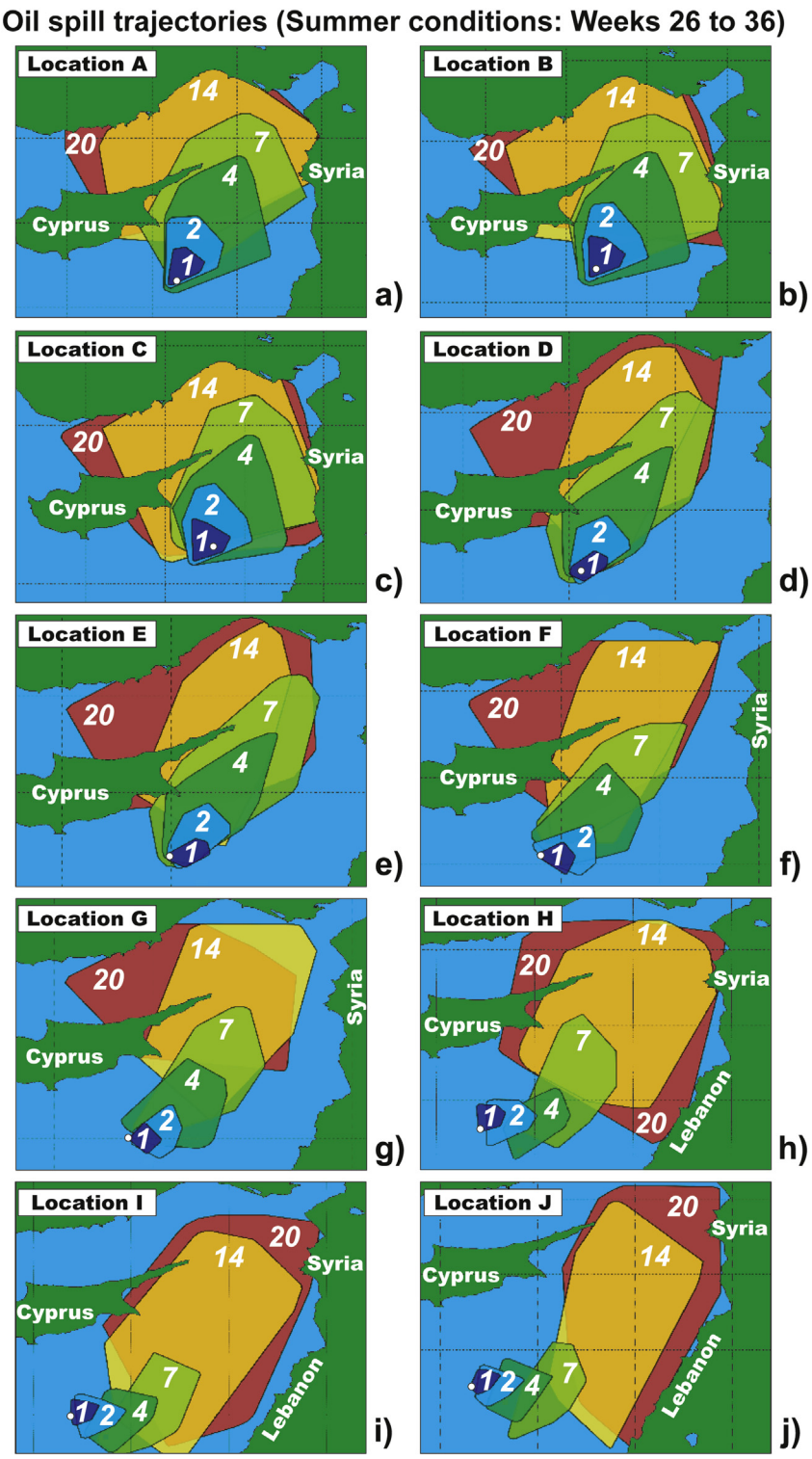

Fig. 5. Superimposed oil spill trajectory maps for T = 1, 2, 4, 7, 14 and 20 days, as computed on MEDSLIK. The figure corresponds to summer conditions (weeks 26–36).

procedures, overstretching the civil protection teams through a large area (see Supplementary Fig. 2).

In order to exemplify the importance of regional current eddies in the Eastern Mediterranean we went a step forward and model the fate of spilt oil under specific, but seasonal, conditions at the Aphrodite field, located in concession Block 12 between Cyprus and Israel (Fig. 1a and b). The oil used for the simulation at the Aphrodite Field was the high-density Belayim Oil (API 21.5°) produced in the Gulf of Suez, spilling at a rate of 8000 m^3/day, with the MEDSLIK simulation running for 50 days. Under late spring conditions (01 June to 30 June 2013), for average wind velocities of 1.7 m/s blowing in a southerly direction, surface currents result in widespread scattering of oil slicks, which will follow the distribution of current eddies in the region (Fig. 1b).

Based on the data in Figs. 1b and 3, it is clear that the use of dispersants is appropriate in oil spill accidents that release large quantities of oil south of Cyprus. The graph in Fig. 3b, for instance, suggests that only ~48% of oil spilt is bound to evaporate in the first 20 days after the spill accident, resulting in the spreading of 52% volume of oil and the potential contamination of a large stretch of the Eastern Levantine Basin if the oil is to disperse freely. Clear advantages in using oil dispersants in the few hours after the spill result from: a) the larger area dispersants potentially treat when combined with mechanical methods; b) limited availability of mechanical equipment and limitations to their use in rough seas, c) the speed in which dispersants can be deployed by aerial means when compared with mechanical equipment. Dispersants have also the advantage of being potentially deployed near the shore, usually >3 nm and at water depths >10 m, with little environmental damage resulting from this deployment if tides and coastal currents provide sufficient dilution to ensure rapid fall in oil concentration. Lessard and DeMarco (2000) state that negative impacts of untreated oil coming ashore are often worse than any impact resulting from the chemical dispersion of oil. Nevertheless, complications may arise when using dispersants. After the Deepwater Horizon oil spill, Kujawinski et al. (2011) showed an ingredient of the dispersant, dioctyl sodium sulfosuccinate (DOSS) to have been sequestered in deepwater hydrocarbon plumes at 1000–1200 m water depth, with its concentration distribution having persisted up to 300 km from the well, 64 days after deepwater dispersant applications ceased. In this case, the authors suggested that negligible, or slow, rates of biodegradation in the affected waters contributed to a high persistence of DOSS in the Gulf of Mexico waters, providing evidence that future toxicological studies should take into account the behaviour of specific dispersant elements when transported by deepwater and surface currents. This is a point under debate, as recent data considers that, in most cases, the potential environmental costs of adding chemicals to a polluted area are outweighed by the much shorter residence time, and hence integrated environmental impact of the spilt oil in the environment (Prince, 2015). The argument is for dispersed oil to degrade much more rapidly than undispersed oil, being also concentrated in one specific area by mechanical and chemical methods (Prince, 2015).

In agreement with the findings in Lessard and DeMarco (2000) and Prince (2015), this paper states that early mitigation procedures are paramount to controlling oil slicks offshore Cyprus. We suggest in this work that the combined action of booms and dispersants will result in no relevant pollution of the coastline if chemical spraying is undertaken at a proper scale early in the oil spill accident i.e., in the first 2–3 days after the accident and mechanical methods are used to clean (and confine) oil close to shoreline booms (see Prince, 2015 for a recent review of oil spill dispersants). In such a setting, dispersant use must occur very quickly after the initial oil release because dispersants are relatively ineffective once weathering and emulsification begin (e.g. Place et al., 2014; Prendergast and Gschwend, 2014; Kleindienst et al., 2015).

6. Conclusions

A total of 104 oil spill simulations, computed for 11 different locations, were combined with bathymetric, meteorological, oceanographic, and geomorphological data in this paper to conclude that:

a) Oil slicks will spread in the Levantine Basin to reach the eastern coast of Cyprus in four (4) to seven (7) days during summer, and eight (8) to fourteen (14) days in winter conditions. Oil spilt will impact the Eastern Mediterranean shores for a period of time that exceeds 20 days, if mitigation techniques are not effective.
b) Oil slick trajectories are chiefly controlled by variable winds and current eddies, justifying the use of chemical dispersants in the very few hours after large accidental oil spills. Local meteorological and current conditions should be also modelled when oil slicks approach the shore.
c) This work shows shoreline susceptibility to vary significantly depending on differences in its morphology, degree of exposure to wave action, and on the existence of uplifted wave-cut platforms, coastal lagoons and pools. The added presence of tourist and environmentally sensitive zones suggests mitigation work should take into account the high shoreline susceptibility of parts of the Eastern Mediterranean Sea.

Emergency teams should use the results shown in this paper to select the best practices to reduce the effects of oil spills. In order to assist them, we show in this paper that Syria, Turkey and Cyprus comprise regions that will suffer the larger impact when an offshore oil spill reaches the shore. We also suggest that the best procedure in distal offshore oil spills will be to use chemical dispersants and booms, i.e. with dispersants being deployed by airplane or locally using pre-equipped vessels.

Acknowledgements

This work has been co-financed by the EU Humanitarian Aid and Civil Protection under Grant Agreement No. 638494/2012/ECHO/A5/SUB Project NEREIDS “Embracing Innovation for Preparedness in Civil Protection & Marine Pollution”'. Part of this work was supported by FP7 MyOcean2 and H2020 MyOcean-FO projects (myocean.org.eu), MED Programme MEDESS-4MS project (medess4ms.org.eu), RAOP-Med (raop.eu) and ENI Cyprus. We also thank the EMODNET MedSea checkpoint project (www.emodnet.eu/med-sea). A special thanks to Mr. Andreas Nicolaides, Mr. Stavros Stylianou and Mrs. Xenia Panayidou at the Cyprus Oceanography Center for contributing in the oceanographic and oil spill data preparation. Two anonymous reviewers and ENVPOL editor Jay Gan provided constructive comments to this work.

Appendix A. Supplementary data

Supplementary data related to this article can be found at http://dx.doi.org/10.1016/j.envpol.2015.07.042.

References

Adler, E., Inbar, M., 2007. Shoreline sensitivity to oil spills, the Mediterranean coast of Israel: assessment and analysis. Ocean Coast. Manag. 50, 24–34.
Alves, T.M., Kokinou, E., Zodiatis, G., Lardner, R., 2016. Hindcast, GIS and susceptibility modelling to assist oil spill clean-up and mitigation on the southern coast of Cyprus (Eastern Mediterranean). In: De Dominicis, M., Ribotti, A. (Eds.), Physical, Chemical and Biological Observations and Modelling of Oil Spills in the Mediterranean Sea. Deep-sea Research II (in press).
Anderson, C.M., LaBelle, R.P., 2000. Update of comparative occurrence rates for offshore oil spills. Spill Sci. Technol. Bull. 5/6, 303–321.
Atlas, R.M., Hazen, T.C., 2011. Oil biodegradation and bioremediation: a tale of the two worst spills in U.S. history. Environ. Sci. Technol. 45, 6709–6715.
Berthou, P., et al., 2008. EMODNET-the European Marine Observation and Data Network. European Science Foundation – Marine Board, p. 10.
Burgherr, P., 2007. In-depth analysis of accidental oil spills from tankers in the context of global spill trends from all sources. J. Hazard. Mater. 1–2, 245–256.
Chrastansky, A., Calles, U., 2009. Model-based long-term reconstruction of weather-driven variations in chronic oil pollution along the German North Sea coast. Mar. Pollut. Bull. 58, 967–975.
Ciappa, A., Costabile, S., 2014. Oil spill hazard assessment using a reverse trajectory method for the Egadi marine protected area (Central Mediterranean Sea). Mar. Pollut. Bull. 84, 44–55.
Coppini, G., De Dominicis, M., Zodiatis, G., Lardner, R., Pinardi, N., Santoleri, R., Colella, S., Bidnami, F., Hayes, D.R., Soloviev, D., Georgiou, G., Kallos, G., 2011.

Hindcast of oil-spill pollution during the Lebanon crisis in the Eastern Mediterranean, July–August 2006. Mar. Pollut. Bull. 62, 140–153.
Cucco, A., Sinercha, M., Ribotti, A., Olita, A., Fazioli, L., Perili, A., Sorgente, B., Borghini, M., Schroeder, K., Sorgente, R., 2012. A high-resolution real-time forecasting system for predicting the fate of oil spills in the Strait of Bonifacio (Western Mediterranean Sea). Mar. Poll. 64, 1186–1200.
Doerffer, J.W., 1992. Oil spill response in the marine environment. Sci. Technol. 395.
El-Bana, M., Khedr, A.-H., Van Hecke, P., Bogaert, J., 2002. Vegetation composition of a threatened hypersaline lake (Lake Bardawil), North Sinai. Plant Ecol. 163, 63–75.
Fingas, M., 2011. Weather Effects on Oil Spill Countermeasures, vol. 13. Gulf Professional Publications, pp. 339–426.
Galanis, G., Hayes, D., Zodiatis, G., Chu, P.C., Kuo, Y.-H., Kallos, G., 2012. Wave height characteristics in the Mediterranean Sea by means of numerical modeling, satellite data, statistical and geometrical techniques. Mar. Geophys. Res. 33, 1–15.
Gille, S.T., Metzger, E.J., Tokmakian, R., 2004. Topography and ocean circulation. Oceanography 17, 47–54.
Giziakis, K., Kanellopoulos, N., Gialoutsi, S., 2013. Spatial analysis of oil spills from marine accidents in Greek waters. SPOUDAI J. Econ. Bus. 63, 60–74.
González, J.J., Viñas, L., Franco, M.A., Fumega, J., Soriano, J.A., Grueiro, G., Muniategui, S., López-Mahía, P., Prada, D., Bayona, J.M., Alzaga, R., Albaigés, J., 2006. Spatial and temporal distribution of dissolved/dispersed aromatic hydrocarbons in seawater in the area affected by the prestige oil spill. Mar. Pollut. Bull. 53, 250–259.
Griffa, A., Piterbang, L., Özgökmen, T., 2004. Predictability of Lagrangian particle trajectories: effects of smoothing of the underlying Eulerian flow. J. Mar. Res. 62, 1–35.
Kleindienst, S., Paul, J.H., Joye, S.B., May 6, 2015. Assessing the effects of chemical dispersants on 1 microbial community composition and activity. Nat. Rev. Microbiol. Opin. http://dx.doi.org/10.1038/nrmicro3452.
Kujawinski, E.B., Kido Soule, M., Valentine, D.L., Boysen, A.K., Longnecker, K., Redmond, M.C., 2011. Fate of dispersants associated with the deepwater horizon oil spill. Environ. Sci. Technol. 45, 1298–1306.
Lardner, R., 2013. Medslik v. 5.3.7 User Manual. Oceanography Centre, University of Cyprus.
Lardner, R., Zodiatis, G., 1998. An operational oil spill model in the Levantine Basin (Eastern Mediterranean Sea). Int. Symposium Mar. Pollut. 10, 5–9.
Lardner, R., Zodiatis, G., Hayes, D., Pinardi, N., 2006. Application of the MEDSLIK Oil Spill Model to the Lebanese Spill of July 2006. European Group of Experts on Satellite Monitoring of Sea Based Oil Pollution, European Communities. ISSN, 1018–5593.
Lessard, R.R., DeMarco, G., 2000. The significance of oil spill dispersants. Spill Sci. Technol. Bull. 6, 59–68.
Lu, X., Soomere, T., Stanev, E.V., Murawski, J., 2012. Identification of the environmentally safe fairway in the South-Western Baltic Sea and Kattegat. Ocean. Dyn. 62, 815–829.
Marshall, D., 1995. Influence of topography on the large-scale ocean circulation. J. Phys. Oceanogr. 25, 1622–1635.
Menna, M., Poulain, P.M., Zodiatis, G., Gertman, I., 2012. On the surface circulation of the Levantine sub-basin derived from Lagrangian drifters and satellite altimetry data. Deep-Sea Res. I 65, 46–58.
Metwalli, A.S., Raboh, T.A., Crema, G., Itoua-Konga, F., Bekhiet, A., Salvini, G., El-Farahaty, M.M., 2012. Strategies to unlock the unexploited oil production potential in the Ashrafi Field, Gulf of Suez, Egypt. North Africa Technical Conference and Exhibition. Society of Petroleum Engineers. http://dx.doi.org/10.2118/150896-MS.
Nissen, K.M., Leckebusch, G.C., Pinto, J.G., Renggli, D., Ulbrich, S., Ulbrich, U., 2010. Cyclones causing wind storms in the Mediterranean: characteristics, trends and links to large-scale patterns. Nat. Hazards Earth Syst. Sci. 1379–1391.
Olita, A., Cucco, A., Simeone, S., Ribotti, A., Fazioli, L., Sorgente, B., Sorgente, R., 2012. Oil spill hazard and risk assessment for the shorelines of a Mediterranean coastal archipelago. Ocean Costal Manag. 57, 44–52.
Panagiotakis, C., Kokinou, E., 2015. Linear pattern detection of geological faults via a topology and shape optimization method. IEEE J. Sel. Top. Appl. Earth Observations Remote Sens. 8, 3–11.
Pashardes, S., Christofides, C., 1995. Statistical analysis of wind speed and direction in Cyprus. Sol. Energy 55, 405–414.
Petterson, C.H., Rice, S.D., Short, J.W., Esler, J.L., Bidkin, B.E., 2003. Long-term ecosystem response to the Exxon Valdez oil spill. Science 302, 2082–2086.
Pinardi, N., et al., 2006. The physical, sedimentary and ecological structure and variability of shelf areas in the Mediterranean Sea. Sea 14, 1243–1330.
Place, B.J., Perkins, M.J., Sinclair, E., Barsamian, A.L., Blakemore, P.R., Field, J.A., 2014. Trace analysis of surfactants in corexit oil dispersant formulations and seawater. Deep-Sea Res. II (in press).
POEM Group, 1992. General circulation of the eastern Mediterranean Sea. Earth Sci. Rev. 32, 285–309.
Prendergast, D.P., Gschwend, P.M., 2014. Assessing the performance and cost of oil spill remediation technologies. J. Clean. Prod. 78, 233–242.
Prince, R.C., 2015. Oil spill dispersants: boon or bane? Environ. Sci. Technol. 49, 6376–6384.
REMPEC, 2002. Protecting the Mediterranean against Maritime Accidents and Illegal Discharges from Ships. Gzira, Malta. http://www.rempec.org/admin/store/wyswigImg/file/Information%20resources/Publications/World_Summit_2002_%28E%29_-_light.pdf.
Soomere, T., Viikmäe, B., Delpeche, N., Myrberg, K., 2010. Towards identification of areas of reduced risk in the Gulf of Finland, the Baltic Sea. Proc. Est. Acad. Sci. 59, 156–165.
Soomere, T., Döös, K., Lehmann, A., Markus Meier, E., Murawski, J., Myrberg, K., Stanev, E., 2014. The potential of current- and wind-driven transport for environmental management of the Baltic Sea. AMBIO 43, 94–104.
Thibodeaux, L.J., Valsaraj, K.T., John, V.T., Papadopoulos, K.D., Pesika, N.S., 2011. Marine oil fate: knowledge gaps, basic research, and development needs; a perspective based on the deepwater horizon spill. Environ. Eng. Sci. 28, 87–93.
UNEP/MAP, 2012. State of the Mediterranean Marine and Coastal Environment. UNEP/MAP – Barcelona Convention, Athens, p. 96.
Vinnem, J.-E., 2014. Offshore Risk Assessment. In: Springer Series in Reliability Engineering, vol. 1. Springer-Verlag. http://dx.doi.org/10.1007/978-1-4471-5207-1_4.
Whitehead, J.A., 1998. Topographic control of oceanic flows in deep passages and straits. Rev. Geophys. 36, 423–440.
Zodiatis, G., Drakopoulos, P., Brenner, S., Groom, S., 2005. Variability of the Cyprus warm core Eddy during the CYCLOPS project. Deep-Sea Res. II 52, 2897–2910.
Zodiatis, G., Hayes, D., Gertman, I., Samuel-Rhodes, Y., 2010. The Cyprus warm eddy and the Atlantic water during the CYBO cruises (1995–2009). Rapports Commun. Int. de la Mer Meditteranee 39, 202.
Zodiatis, G., Hayes, D., Gertman, I., Poulain, P.-M., Menna, M., Nicolaidis, A., 2013. On the main flow features of the SE Levantine (CYBO cruises 1995–2012). Geophys. Res. Abstr. 15, EGU2013–9861.
Zodiatis, G., Lardner, R., Solovyov, D., Panayidou, X., De Dominicis, M., 2012. Predictions of oil slicks detected from satellite images using MyOcean forecasting data. Ocean Sci. 8, 1105–1115.
Zodiatis, G., Galanis, G., Nikolaidis, A., Kalogeri, C., Hayes, D., Georgiou, G., Chu, P.C., Kallos, G., 2014. Wave energy potential in the eastern mediterranean Levantine Basin. An integrated 10-year study. Renew. Energy 69, 311–323. http://dx.doi.org/10.1016/j.renene.2014.03.051.